Metamaterial engineered C+L band 90º hybrid with 150 nm feature size

Abdelfettah Hadij-ElHouati, [1,*] Robert Halir,[1] Alejandro Ortega-Moñux,[1] J. Gonzalo Wangüemert-Pérez,[1]
Hugh Podmore,[2] Jens H. Schmid,[3] Pavel Cheben,[3,4] and Iñigo Molina-Fernandez[1]

[1]*Departamento de Ingeniería de Comunicaciones, ETSI Telecomunicación, Universidad de Málaga, Campus de Teatinos s/n, 29071 Málaga, Spain*
[2]*Honeywell Aerospace, 303 Terry Fox Dr., Ottawa, Ontario K2K 3J1, Canada*
[3]*National Research Council Canada, Ottawa, Ontario K1A 0R6, Canada*
[4]*Center for Research in Photonics, University of Ottawa, Ottawa K1N6N5, Canada*
*Corresponding author: abdel@uma.es

***Abstract*—90º hybrids are important components for coherent optical communications. Conventional implementations only cover the C band, while broadband, metamaterial-based devices require sub-100nm feature sizes. We propose a design based on dual-etch silicon subwavelength structures that achieves a 170 nm bandwidth with deep-UV compatible feature sizes.**

Keywords—MMI, SOI, SWG, 90º hybrid, coherent receiver

I. Introduction

High bandwidth optical communications require advanced, coherent modulation formats, that rely on the retrieval of both the amplitude and phase of the received optical signal [1]. For this purpose, the preferred solution, in terms of both simplicity and robustness, is using a 2×4 hybrid and balanced photodiodes. The hybrid combines the received signal and the local laser with four different relative phases. By feeding the output of the hybrid into photodiodes, amplitude and phase (i.e. I and Q components) of the optical signal can be retrieved [Fig. 1(a)].

Multimode interferometers (MMI) are the preferred device for implementing 2×4 hybrids because they do not require any active tuning. Conventional MMI implementations in silicon on insulator (SOI) exhibit a limited operational bandwidth of ~40 nm that covers only the C band [2]. Subwavelength grating (SWG) metamaterial engineering has been successfully used to improve the performance of a myriad of photonics devices [3]. SWGs have been successfully used to substantially enlarge the bandwidth of MMI devices, albeit at the expense of reducing the minimum feature size (MFS) [4], [5]. For instance, the hybrid reported in [5] has an MFS of 111 nm. However, for a device to transcend research labs and possibly reach the market it needs to be mass-producible with deep ultraviolet (DUV) stepper lithography. To achieve a practical fabrication yield using conventional (DUV) lithography, feature sizes significantly larger than 100 nm are desirable.

Many modern silicon fabrication platforms already implement multiple etch steps to accommodate devices such as fiber-to-chip grating couplers and modulator contacts [6]. In this work we harness this extra degree of freedom to overcome the tradeoff between bandwidth and minimum feature size in MMI-based hybrids using the geometry shown in Fig. 1(b). As a result, we achieve an excellent performance over a remarkable bandwidth of 170 nm maintaining a large minimum feature size of 150 nm, which is suitable for DUV lithography.

II. Operational Principle

MMI operation is based on the self-imaging effect in a multimode waveguide capable of reproducing an input field in several images at specific propagation distances. In a 2×4 MMI the first four-fold image of the input field forms at the distance [7]:

$$L_{MMI} = \frac{3L_\pi(\lambda)}{4}, \tag{1}$$

where L_{MMI} is the physical length of the device, λ is the free space wavelength and L_π is the beat-length of the two first modes in the multimode region:

$$L_\pi(\lambda) = \frac{\lambda}{2(n_{\mathrm{eff}}^0(\lambda) - n_{\mathrm{eff}}^1(\lambda))}, \tag{2}$$

where n_{eff}^0 and n_{eff}^1 are the effective indexes of the first and second order mode, respectively. Because of the wavelength dependence of the beat length, Eq. (1) holds for a limited bandwidth. Thus, in order to achieve broadband behavior, $L_\pi(\lambda)$ dependence with wavelength needs to be minimized. This can be achieved with a judiciously engineered anisotropic metamaterial in the MMI region [4], but requires a small period to avoid the Bragg regime, i.e. $\Lambda_z < \lambda/(2n_{\mathrm{eff}}^0)$, which in turn results in small feature sizes. Here, we exploit a dual-etch process to reduce the overall equivalent index in the multimode region thereby increasing the minimum feature size while maintaining a high bandwidth.

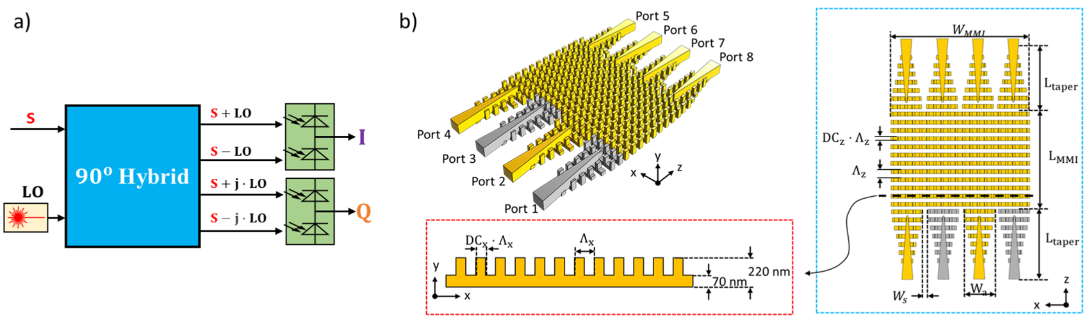

Fig. 1. a) Coherent optical receiver based on a 90º hybrid that combines the received signal S with the local oscillator (LO). b) Geometry of the proposed 2 × 4 MMI hybrid, that uses a two-etch-step SWG metamaterial to synthesize an anisotropic material to achieve a broad bandwidth and a large feature size.

III. Design and Simulations

Figure 1(b) shows the schematic of the proposed device, operating in TE (in-plane) polarization. We assume a silicon-on-insulator platform with 2 µm silicon dioxide buried oxide, 2 µm silicon dioxide upper cladding and a 220 nm thick silicon layer, that can be etched either fully, or leaving a 70 nm thick silicon slab.

The input and the output waveguides are widened to 1.7 µm to ensure low insertion loss and imbalance using a 15.6-µm-long taper [4]. The input and the output waveguides are separated by $W_s = 0.7$ µm to suppress crosstalk. The MMI width W_{MMI} is set to 9.4 µm to fit the four ports while keeping the device as compact as possible.

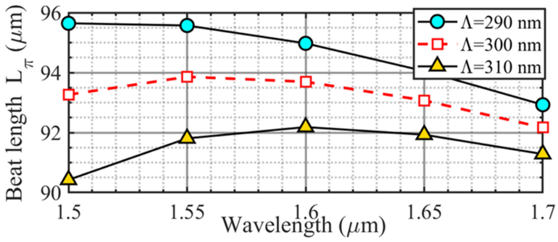

Fig. 2. Beat length of the two first modes in the MMI region as a function of the wavelength for various periods in the z direction and $\Lambda_x = 300$ nm.

The MMI subwavelength grating parameters (DC_x , DC_z, Λ_x and Λ_z) were designed to obtain maximum MFS and bandwidth. First, we set $DC_x = 0.5$, $DC_z = 0.5$ and $\Lambda_x = 300$ nm to obtain the target MFS (150 nm) in the *x* direction and maximize the MFS in the *z* direction. Finally, we design the longitudinal period Λ_z to flatten the $L_\pi(\lambda)$ curve, thereby maximize the bandwidth. For this purpose, we employed an efficient Floquet-Bloch mode analysis of just one longitudinal period using a 3D FDTD simulator that supports periodic boundary conditions and spectral analysis techniques [8]. As shown in Fig. 2, for a period of 300 nm we achieve the flattest wavelength behavior of $L_\pi(\lambda)$ within the 1.5 µm – 1.6 µm band, while still maintaining a large feature size of 150 nm. This results in an MMI region length of $L_{MMI} = 3L_\pi/4 = 69.9$ µm.

To assess device performance a 3D FDTD simulation of the complete structure shown in Fig. 1(b) was carried out. Figure 3 shows the relevant figures of merit, namely the insertion loss, the common mode rejection ratio (CMRR) and phase error as defined in [9], confirming that our device meets telecom industry requirements in a bandwidth of 170 nm [10].

IV. Conclusion

A new type of 2×4 90º hybrid based on multimode interference was proposed based on metamaterial index engineering. 3D FDTD simulation demonstrated that the proposed design has a good performance (insertion loss < 1 dB, CMRR< -20 dBe and phase error < 5º) over a remarkable bandwidth of 170 nm. Moreover, the minimum feature size is 150 nm which makes it compatible with mass production using deep UV lithographic process.

Acknowledgment

This work was supported by the *Spanish Ministerio de Universidades (FPU-16/03401); Ministerio de Economía y Competitividad FEDER (TEC2016-80718-R); Programa Operativo FEDER Andalucía 2014-2020 (UMA18-FEDERJA-219);* and *Universidad de Malaga*.

References

[1] C. Doerr and L. Chen, "Silicon Photonics in Optical Coherent Systems," *Proc. IEEE*, vol. 106, no. 12, pp. 2291–2301, Dec. 2018.

[2] H. Guan *et al.*, "Compact and low loss 90° optical hybrid on a silicon-on-insulator platform," *Opt. Express*, vol. 25, no. 23, p. 28957, Nov. 2017.

[3] P. Cheben, R. Halir, J. H. Schmid, H. A. Atwater, and D. R. Smith, "Subwavelength integrated photonics," *Nature*, vol. 560, no. 7720, pp. 565–572, Aug. 2018.

[4] R. Halir *et al.*, "Ultra-broadband nanophotonic beamsplitter using an anisotropic sub-wavelength metamaterial," *Laser Photon. Rev.*, vol. 10, no. 6, pp. 1039–1046, Nov. 2016.

[5] L. Xu *et al.*, "Ultra-broadband and ultra-compact optical 90° hybrid based on 2×4 MMI coupler with subwavelength gratings on silicon-on-insulator," *2018 Opt. Fiber Commun. Conf. Expo. OFC 2018 - Proc.*, pp. 1–3, 2018.

[6] M. Pantouvaki *et al.*, "Active Components for 50 Gb/s NRZ-OOK Optical Interconnects in a Silicon Photonics Platform," *J. Light. Technol.*, vol. 35, no. 4, pp. 631–638, Feb. 2017.

[7] L. B. Soldano and E. C. M. Pennings, "Optical Multi-Mode Interference Devices Based on Self-Imaging: Principles and Applications," *J. Light. Technol.*, vol. 13, no. 4, pp. 615–627, 1995.

[8] A. Hadij-ElHouati *et al.*, "Distributed Bragg deflector coupler for on-chip shaping of optical beams," *Opt. Express*, vol. 27, no. 23, p. 33180, Nov. 2019.

[9] R. Halir, G. Roelkens, A. Ortega-Moñux, and J. G. Wangüemert-Pérez, "High-performance 90° hybrid based on a silicon-on-insulator multimode interference coupler," *Opt. Lett.*, vol. 36, no. 2, p. 178, 2011.

[10] Optical Internetworking Forum, "Implementation Agreement for Integrated Dual Polarization Micro-Intradyne Coherent Receivers." 2015.

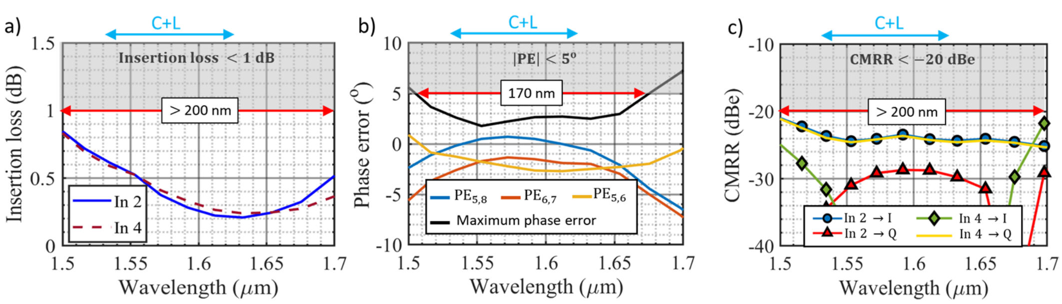

Fig. 3. a) Insertion loss, b) relative phase error and c) CMRR of the designed hybrid obtained by 3D FDTD simulation of the whole device. Grey areas indicate regions in which telecom industry requirements [10] are not met.